Appl Phys A (2013) 111:907–912
DOI 10.1007/s00339-012-7311-x

Applied Physics A
Materials Science & Processing

Structure and multiferroic properties of Eu-substituted $BiFeO_3$ ceramics

Haiyang Dai · Zhenping Chen · Renzhong Xue · Tao Li · Haizeng Liu · Yongqiang Wang

Received: 3 July 2012 / Accepted: 4 October 2012 / Published online: 17 October 2012

Abstract Polycrystalline $Bi_{1-x}Eu_xFeO_3$ ($x = 0.00$–0.25) ceramics were synthesized by the solid state reaction method with the rapid liquid phase sintering process. The effects of Eu substitution on the structure, and ferroelectric and magnetic properties of $BiFeO_3$ ceramics were investigated. X-ray diffraction measurements reveal that the structure of $BiFeO_3$ was changed from rhombohedral to orthorhombic and the impurity phases were decreased both due to Eu substitution. Raman spectra results also confirm that a structure transition occurs in the Eu concentration range of 0.15–0.20. The SEM investigation has suggested that the Eu substitution hinders the grain growth. Vibrating sample magnetometer measurements indicate ferromagnetism in Eu-substituted $BiFeO_3$ ceramics. It is found that the room temperature magnetic moment increases with increasing Eu concentration due to the suppressed or broken cycloid spin structure. Ferroelectric measurements show that Eu substitution enhances the polarization due to the significant decrease of the electric leakage of the samples. Therefore, the Eu-substituted $BiFeO_3$, or more complicated substituted $BiFeO_3$ based on Eu substitution, will have great potential for many practical applications.

1 Introduction

Multiferroic materials are such a kind of material that possess simultaneously ferroelectric and ferromagnetic as well as magnetoelectric properties, hence they will have many potential applications in the information storage, spintronic devices, sensors, and so on areas [1, 2]. Among them, $BiFeO_3$ (BFO) with a rhombohedrally distorted perovskite structure of R3c is the only known single phase material which exhibits ferroelectric and antiferromagnetic orders at room temperature and a coexistence of ferroelectric and antiferromagnetic orders at ferroelectric Curie temperature T_C of ∼830 °C and at the antiferromagnetic Néel temperature T_N of ∼370 °C [2, 3]. Such a material has been widely studied by many groups due to its importance in fundamental research as well as in potential commercial applications.

However, there are still some drawbacks that need to be overcome before $BiFeO_3$ can be used in devices. For one, it is difficult to gain a good polarization hysteresis (P-E) loop and large remnant polarization (Pr) in $BiFeO_3$ ceramics because its leakage current is high and its resistance is low due to the fact that there are secondary phases and oxygen vacancies in it [4–6]. For another, $BiFeO_3$ with a G-type antiferromagnetic spin structure, and a superimposed and cycloidal modulation at a period of about 62 nm can lead to superimposing on the antiferromagnetic ordering, and hence can result in the cancellation of net magnetization [4, 5]. Its very weak magnetization inhibits the observation of the linear magnetoelectric effect [4]. Therefore, considerable efforts such as ion substitution have been made to improve the room temperature multiferroic properties of $BiFeO_3$ ceramics. For example, attempts have been made to improve the magnetic and ferroelectric properties of $BiFeO_3$ by substituting the Bi-site with La, Nd atoms and the Fe-site with Cr, Mn, and Ti atoms, etc. [1–11]. In this study, we report the synthesis of $BiFeO_3$ ceramics doped by Eu^{3+} for partial Bi^{3+}. The effect of Eu substitution on the structural, ferroelectric and magnetic properties of $BiFeO_3$ ceramics was investigated.

H. Dai · Z. Chen (✉) · R. Xue · T. Li · H. Liu · Y. Wang
Department of Technology and Physics, Zhengzhou University of Light Industry, Zhengzhou 450002, China
e-mail: haiyangdai@126.com
Fax: +86-371-63556150

2 Experimental details

The polycrystalline ceramics samples of $Bi_{1-x}Eu_xFeO_3$ ($x = 0.00, 0.10, 0.15, 0.20, 0.25$) were prepared using a solid state reaction method with the rapid liquid phase sintering process. High purity analytical powders of Bi_2O_3 (99.999 %), Eu_2O_3 (99.99 %), and Fe_2O_3 (99.99 %) were used as starting materials. Those powders were carefully weighed and in stoichiometric proportions (3 % bismuth excess to compensate the Bi loss) and ground thoroughly in an agate mortar for 6 h using ethanol as a medium. The mixed powders were dehydrated at 150 °C for 12 h and dry pressed into small discs with 11 mm in diameter and 1.6 mm in thickness at 16 MPa pressure. The disks were directly put into a furnace, and then sintered at 850–880 °C with an accuracy of ±1 °C for 20 min. After that, they were taken out of the furnace immediately and quenched subsequently to room temperature. The polished flat surfaces of these samples were coated with silver paste and dried at 550 °C for 30 min before taking electrical measurements.

The structures of samples were studied by Bruke D8 X-ray diffraction (XRD) with Cu-K_α radiation. Raman measurements were carried out at room temperature using a Renishaw inVia spectrometer, and the excitation source was the 514.5 nm line of an Ar^+ laser with 200 mW output. The power of the laser spot on the sample was less than 20 mW to prevent laser heating damages. The fracture surface of the samples was carried out in a scanning electron microscope (SEM). The magnetization of the samples was measured by a vibrating sample magnetometer integrated in a magnetic property measurement system (MPMS, Quantum Design). The ferroelectric properties of $Bi_{1-x}Eu_xFeO_3$ ceramics were measured using a RT 6000 ferroelectric tester and all the measurements were carried out at room temperature.

3 Results and discussion

The XRD patterns of $Bi_{1-x}Eu_xFeO_3$ ceramics at room temperature are illustrated in Fig. 1. XRD peak intensity ratios observed in the above XRD pattern suggest polycrystalline behavior with good crystallinity. A rhombohedral perovskite structure with the space group R3c can be indexed in the pattern of the unsubstituted $BiFeO_3$ [1, 3]. A small amount of impurity phases such as $Bi_2Fe_4O_9$ and $Bi_{25}FeO_{39}$ is also detected in the unsubstituted $BiFeO_3$ ceramics [1, 5]. It is also found that the impurity phases in $Bi_{1-x}Eu_xFeO_3$ ceramics decrease with increasing Eu content, and they almost disappear when the Eu content increases up to $x \geq 0.2$. Based on the XRD patterns with different Eu content samples, it is found that the peaks within 2θ of 20∼25° and 30∼35° shift to a higher angle side when x is increased. This indicates that Eu^{3+} ions have entered into the $BiFeO_3$ lattice

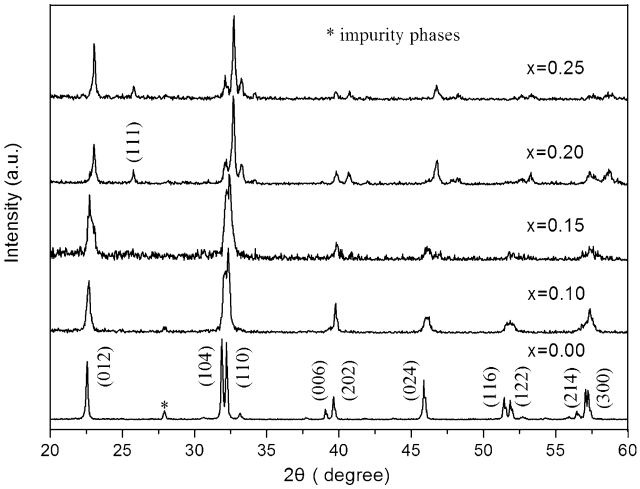

Fig. 1 XRD patterns of $Bi_{1-x}Eu_xFeO_3$ ceramics at room temperature

and substituted for Bi^{3+} ions, which affected the structure of the original crystals of $BiFeO_3$. It is also found that a new (111) peak in the vicinity of $2\theta \approx 27°$ appeared when the Eu concentration increased to $x = 0.15$ and 0.20, respectively. This is evidence of the structural transformation occurrence. The lattice constants a, b, and c of the Eu doped $BiFeO_3$ samples are calculated by the JADE 5.0 program in order to determine their structural features. The lattice parameters, unit cell volume, and crystalline structure of $Bi_{1-x}Eu_xFeO_3$ ceramics are summarized in Table 1. In the present work, the best fit to data is observed using the rhombohedral lattice type for $x = 0.00$, 0.10, and 0.15 samples and with the orthorhombic lattice type for $x = 0.20$ and 0.25 samples. Although the room temperature phase of $BiFeO_3$ is known to be rhombohedral with the R3c space group, the unit cell can also be described in a hexagonal frame of reference [4]. Therefore, in our work, the XRD patterns for the samples with $x = 0.00$, 0.10, and 0.15 are indexed with the space group R3c with a hexagonal unit cell. In Table 1, the refined lattice crystal parameters are $a = 5.57306$ Å, $c = 13.86252$ Å for $x = 0.00$, which agree well with those of the pure $BiFeO_3$ prepared by the solid state reaction method [8], $a = 5.57132$ Å, $c = 13.86146$ Å for $x = 0.10$, $a = 5.57122$ Å, $c = 13.83894$ Å for $x = 0.15$, the parameters of $a = 5.36206$ Å, $b = 5.60036$ Å, $c = 7.68350$ Å for $x = 0.20$, and the ones of $a = 5.37865$ Å, $b = 5.58692$ Å, $c = 7.75840$ Å for $x = 0.25$. It can be found that the values of the parameters a and c decreased slightly with increasing x from 0.00 to 0.15, which result in a slow reduction in volume. When x increases from 0.15 to 0.20, the volume shows a big reduction indicating that the phase transition from the rhombohedral to orthorhombic phase occurs in the Eu concentration range of 0.15–0.20. Such a transition probably resulted from the smaller ionic radius of Eu^{3+} (1.07 Å) than that of Bi^{3+} (1.17 Å) [3]; the change of the lattice constant also confirms the substitution of Bi^{3+} by Eu^{3+}.

Table 1 The lattice parameters and crystalline structure of $Bi_{1-x}Eu_xFeO_3$ ceramics

Sample	a (Å)	b (Å)	c (Å)	V (Å^3)	Crystalline structure
$x = 0.00$	5.57306	5.57306	13.86252	372.87	Rhombohedral
$x = 0.10$	5.57132	5.57132	13.86146	372.62	Rhombohedral
$x = 0.15$	5.57122	5.57122	13.83894	371.99	Rhombohedral
$x = 0.20$	5.36206	5.60036	7.68350	230.73	Orthorhombic
$x = 0.25$	5.37865	5.58692	7.75840	233.14	Orthorhombic

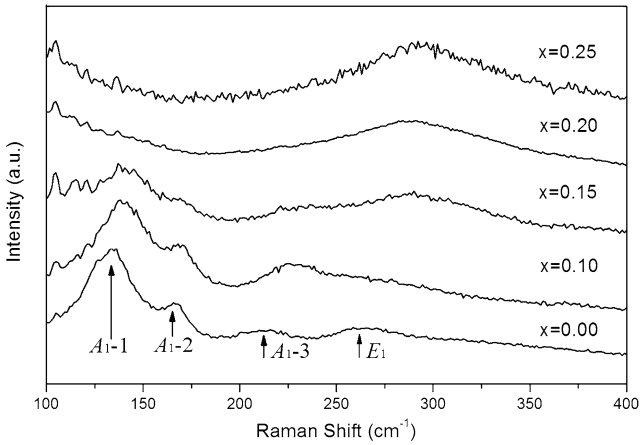

Fig. 2 Raman spectra of $Bi_{1-x}Eu_xFeO_3$ samples

Raman spectroscopy is a powerful tool to probe the structural and vibrational property of a material [2, 13]. Room temperature Raman spectra of $Bi_{1-x}Eu_xFeO_3$ samples in the range of 100–400 cm^{-1} are shown in Fig. 2. In the present study, four fundamental Raman modes can be seen in the spectrum of an unsubstituted $BiFeO_3$ sample; the first three peaks located at 135, 165, and 213 cm^{-1} are A_1 modes, recorded as A_1-1, A_1-2, A_1-3, respectively. And the remaining peak located at 261 cm^{-1} is the E mode [14–16]. The mode frequencies are in good agreement with other reports [7, 14, 15]. The intensity of A_1-1 and A_1-2 modes is strong, while the intensity of the A_1-3 mode and E mode is relatively weak. Since Raman scattering spectra are sensitive to atomic displacements, the evolvement of Raman normal modes with an increasing Eu content can provide valuable information about ionic substitution, phase transitions, and electric polarization [7, 16]. The polarization of $BiFeO_3$ generally originates from the stereochemical activity of the Bi ion lone pair electron that is mainly responsible for the change in both Bi–O covalent bonds. The four characteristic modes, i.e., A_1-1, A_1-2, A_1-3, and E are believed to be responsible for the polarization of the $BiFeO_3$ samples. It can be seen from Fig. 2 that when x increases from 0.00 to 0.15, the A_1-1, A_1-2, and A_1-3 modes shifted to higher mode frequencies; the mode intensity had a continuous and slow change. These displacements indicate that the Eu atom substitutes Bi into the $BiFeO_3$ site. In the $Bi_{1-x}Eu_xFeO_3$ samples, with the replacement of Eu^{3+} for Bi^{3+}, a part of Bi–O bonds were replaced by Eu–O bonds and the stereochemical activity of the Bi lone electron pair was changed. The Eu^{3+} ion with smaller size and lighter mass replaced for the Bi^{3+} ion may cause a decline of the stereochemical activity of the Bi lone electron pair and change the Bi–O bonds, and then affect the polarization of the samples [3, 12]. And the presence of the A-site ion disorder commonly brings a continuous and slow change for mode intensity [12]. When x increases from 0.15 to 0.20, the most important feature in the Raman spectra is the peaks of A_1-2 and A_1-3 modes almost vanishes. It also can be seen that the A_1-1 mode severely broadens and shifted to lower mode frequencies, while the E mode shifted to higher mode frequencies and its intensity increased. The reduced phonon modes and the changes in characteristic peaks suggest that a phase transition happened when the Eu concentration increased to the range of 0.15–0.25 [7]. This is consistent with the XRD results.

Figure 3 shows the fracture surface SEM images of $Bi_{1-x}Eu_xFeO_3$ samples. It can be seen that the unsubstituted $BiFeO_3$ sample mainly consists of large grains with spherical pores inside the grains, which appeared to grow abnormally or discontinuously. The morphologies show that the grain size became small and surface density became large with increasing the Eu content for the $Bi_{1-x}Eu_xFeO_3$ system. The decrease in grain size may be attributed to the difference in the ionic radius of Bi^{3+} and Eu^{3+} and variation in bond strength [17, 18].

To investigate the magnetic properties of $Bi_{1-x}Eu_xFeO_3$ ceramics, magnetic measurements are performed. Figure 4 shows the magnetization hysteresis (M–H) loops of $Bi_{1-x}Eu_xFeO_3$ ceramics at room temperature. The M–H loops of the pure $BiFeO_3$ ceramics showed insignificant magnetization with almost no spontaneous magnetization. However, the loops for the $x = 0.10$, 0.20, and 0.25 samples showed clear magnetic characteristics. The partly enlarged M–H loop for the unsubstituted $BiFeO_3$ ceramics ($x = 0.00$) is presented in the inset (a) in Fig. 4, where a nonzero but small remnant magnetization (Mr) of 7.2×10^{-4} emu/g, together with a coercive field (Hc) of 0.5 kOe is achieved. Such a small remnant magnetization in the unsubstituted samples might come from a small amount of other impurity phases, such as Fe oxides [10]. The insert (b) of Fig. 4 shows the partly enlarged hysteresis loops of Eu-substituted $BiFeO_3$, where the values of saturation magnetization (Ms)

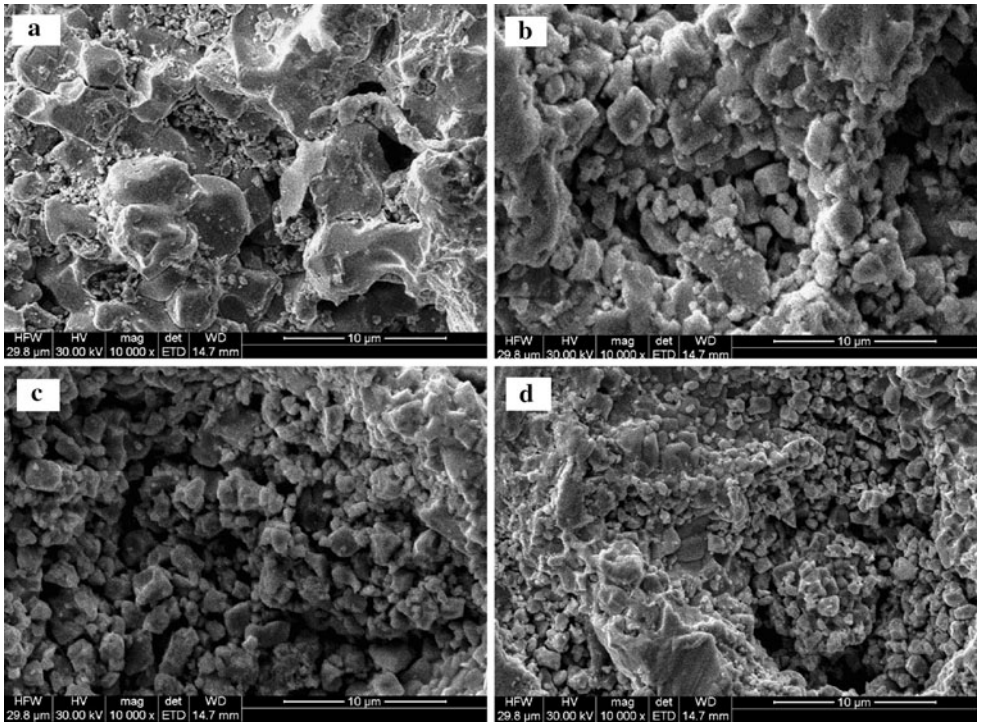

Fig. 3 SEM images of $Bi_{1-x}Eu_xFeO_3$ samples (**a**) $x = 0$, (**b**) $x = 0.10$, (**c**) $x = 0.15$, and (**d**) $x = 0.25$

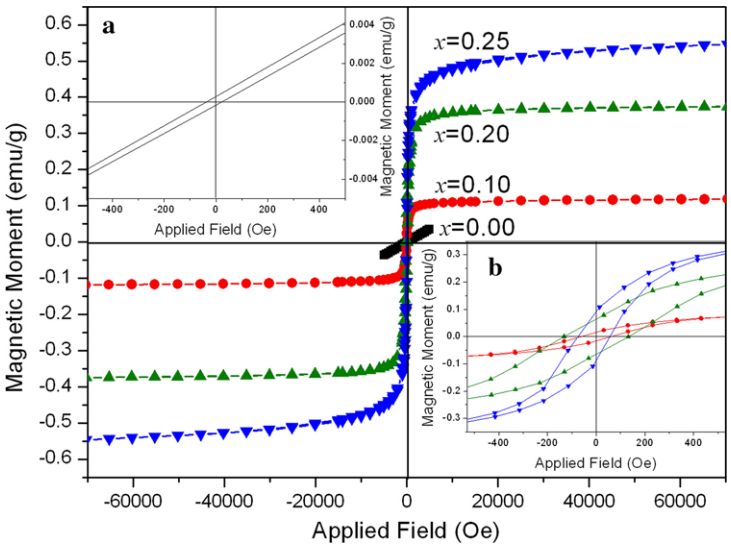

Fig. 4 Magnetization hysteresis (M–H) loops of $Bi_{1-x}Eu_xFeO_3$ ceramics at $T = 300$ K. The inset (**a**) shows the partly enlarged M–H loop for unsubstituted samples. The inset (**b**) shows the partly enlarged M–H loops for Eu-substituted samples

for $x = 0.10$, 0.20, and 0.25 samples are about 0.24, 0.37, and 0.55 emu/g, and the values of Mr are 0.033, 0.065, and 0.094 emu/g, respectively. This means that the increases in the values of Ms and Mr with increasing x from 0.00 to 0.25 are likely due to the Eu substitution for Bi, which can suppress and even destruct the space modulated cycloidal spin structure, and, hence can release the locked magnetization.

The room temperature ferroelectric hysteresis loop for $Bi_{1-x}Eu_xFeO_3$ ceramics is shown in Fig. 5. The loop seems to be unsaturated behavior because of a higher leakage current and partial reversal of polarization. Owing to the low breakdown fields, the maximum applied electric field for unsubstituted $BiFeO_3$ is about 10 kV/cm. The maximum applied electric field for Eu-substituted $BiFeO_3$ is about 40 kV/cm. The value of remnant polarization (2Pr) for the pure $BiFeO_3$ samples is about 0.27 uC/cm^2, while the values of remnant polarization (2Pr) for $x = 0.10$, 0.15, 0.20, and 0.25 samples are about 0.66 uC/cm^2, 1.06 uC/cm^2, 2.78 uC/cm^2, and 1.94 uC/cm^2, respectively. It is obvious that Eu substitution can increase the ferroelectricity of $BiFeO_3$. And the remnant polarization can be enhanced when the Eu content increases from 0.00 to 0.20, but decreased when the Eu content increases from 0.20 to 0.25. It is believed that A site substitution can improve the ferroelectric behavior due to

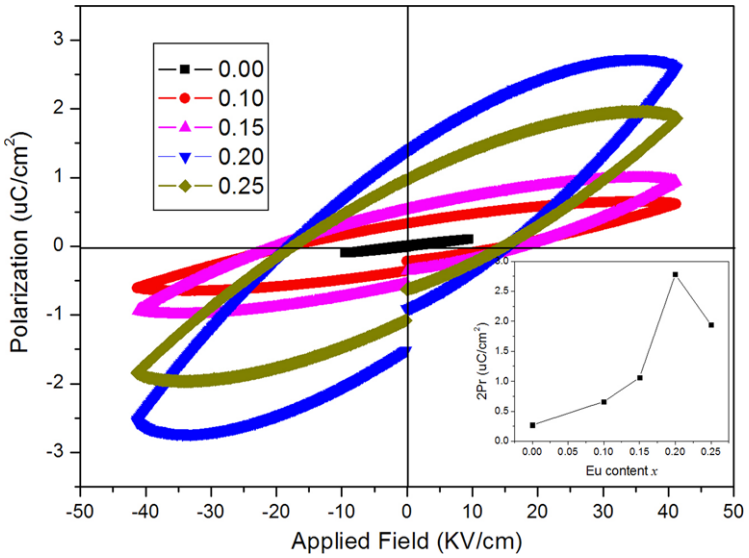

Fig. 5 Ferroelectric hysteresis (P–E) loops of $Bi_{1-x}Eu_xFeO_3$ ceramics at room temperature

the decrease of the leakage current. Based on the results of XRD and Raman measurements, it can be seen that the substitution of Eu for Bi could decrease the impurity phases, change the Bi–O covalent bonds, and strengthen the distortion resulting in the decrease of leakage current density and the enhancement of ferroelectric behavior of $BiFeO_3$. Therefore, the remnant polarization increases with increasing the Eu content from 0.00 to 0.20. Further increase in the Eu content ($x = 0.20$–0.25) would result in a unit cell volume contraction because the ionic radius of Eu^{3+} is smaller than that of Bi^{3+} [3]. And the free volume available for the displacement of Fe^{3+} ions in the Fe–O oxygen octahedral becomes smaller and this would lead to a decrease in polarization. Therefore, the remnant polarization value decreases when the Eu content increases from 0.20 to 0.25.

4 Conclusions

Polycrystalline samples of $Bi_{1-x}Eu_xFeO_3$ ($x = 0$–0.25) ceramics were synthesized by the solid state reaction method with the rapid liquid phase sintering process. The effects of Eu substitution in the $BiFeO_3$ on its structural, ferroelectric, and magnetic behaviors were investigated.

(1) XRD and Raman spectra reveal that a structure transition occurs when the Eu concentration is in the range of 0.15–0.20. The substitution of Eu for Bi can hinder the formation of impurity phases and at the same time influence the Bi–O bonds in the $Bi_{1-x}Eu_xFeO_3$ samples.
(2) SEM morphologies show that the introduction of Eu can hinder the grain growth.
(3) Magnetic measurements indicate that the magnetization hysteresis loops of Eu-substituted samples have a saturated character. It is found that the substitution of Eu for Bi can dramatically improve the saturation magnetization and remnant magnetization.
(4) Ferroelectric measurements show that the remnant polarization for the $Bi_{1-x}Eu_xFeO_3$ samples increases with increasing the Eu content from 0.00 to 0.20, while decreases with increasing the Eu content from 0.20 to 0.25.

Acknowledgements This work was supported by the National Natural Science Foundation of China (Nos. 11175159 and 51002144), the School Doctor Foundation of Zhengzhou University of Light Industry (No. 2010BSJJ030), and The Basic Research Plan on Natural Science of the Science and Technology Department of Henan Province (No. 122102210436).

References

1. S.X. Zhang, W.J. Luo, D.L. Wang, Y.W. Ma, Mater. Lett. **63**, 1820 (2009)
2. A. Kumar, D. Varshney, Ceram. Int. **38**, 3935 (2012)
3. X.Q. Zhang, Y. Sui, X.J. Wang, Y. Wang, Z. Wang, J. Alloys Compd. **507**, 157 (2010)
4. S. Chauhan, M. Kumar, S. Chhoker, S.C. Katyal, H. Singh, M. Jewariya, K.L. Yadav, Solid State Commun. **152**, 525 (2012)
5. J. Liu, M.Y. Li, Z.Q. Hu, L. Pei, J. Wang, X.L. Liu, X.Z. Zhao, Appl. Phys. A **102**, 713 (2011)
6. X.M. Chen, G.H. Wu, H.L. Zhang, N. Qin, T. Wang, F.F. Wang, W.Z. Shi, D.H. Bao, Appl. Phys. A **100**, 987 (2010)
7. V.A. Khomchenko, M. Kopcewicz, A.M.L. Lopes, Y.G. Pogorelov, J.P. Araujo, J.M. Vieira, A.L. Kholkin, J. Phys. D, Appl. Phys. **41**, 102003 (2008)
8. R. Rai, S.K. Mishra, N.K. Singh, S. Sharma, A.L. Kholkin, Curr. Appl. Phys. **11**, 508 (2011)
9. N.V. Minh, D.V. Thang, J. Alloys Compd. **505**, 619 (2010)
10. Z. Wen, X. Shen, D. Wu, Q.Y. Xu, J.L. Wang, A.D. Li, Solid State Commun. **150**, 2081 (2010)
11. A. Kumar, K.L. Yadav, Mater. Sci. Eng. B **176**, 227 (2011)
12. G.L. Yuan, S.W. Or, H.L.W. Chan, J. Appl. Phys. **101**, 064101 (2007)

13. A. Kumar, N.M. Murari, R.S. Katiyar, J. Raman Spectrosc. **39**, 1262 (2008)
14. P. Rovillain, M. Cazayous, A. Sacuto, D. Lebeugle, D. Colson, J. Magn. Magn. Mater. **321**, 1699 (2009)
15. A. Gautam, K. Singh, K. Sen, R.K. Kotnala, M. Singh, Mater. Lett. **65**, 591 (2011)
16. C.M. Wang, H.Y. Dai, T. Li, R.Z. Xue, L. Su, Z.P. Chen, Adv. Mater. Res. **239–242**, 1501 (2011)
17. J.A. Dean, *Lange's Handbook of Chemistry*, 15th edn. (McGraw-Hill, New York, 1999), pp. 4.42–4.45
18. A. Gautam, K. Singh, K. Sen, R.K. Kotnala, M. Singh, J. Alloys Compd. **517**, 87 (2012)